Study of Polystyrene and Acrylonitrile−Styrene Copolymer as Special β-Nucleating Agents To Induce the Crystallization of Isotactic Polypropylene

Zhiqiang Su, Mu Dong, Zhaoxia Guo, and Jian Yu*

Institute of Polymer Science and Engineering, Department of Chemical Engineering, School of Materials Science and Engineering, Tsinghua University, Beijing 100084, China

Received October 13, 2006; Revised Manuscript Received April 13, 2007

ABSTRACT: The influence of two kinds of polymers (polystyrene (PS), acrylonitrile−styrene copolymer (SAN)) on the crystallization behavior of isotactic polypropylene (iPP) has been investigated by means of wide-angle X-ray diffraction (WAXD), differential scanning calorimetry (DSC), and polarized optical microscopy (POM). The current experimental results indicated that these two kinds of polymers with low concentration, as special β-nucleating agents, can induce the β-iPP polymorph during quiescent melt crystallization. The nucleating activity of SAN or PS significantly depends on its concentration, molecular structure, and thermal history of processing. The content of β-crystal form increases with the increasing crystallization temperature or nucleating agent (SAN or PS) percentage, reaches a maximum value, and then decreases as the temperature or nucleating agent percentage further increases. Under the same crystallization condition, SAN is more effective than PS on inducing a higher level of β-crystal form in iPP. Besides, variable temperature WAXD and POM experiments have been used to investigate the polymorphism and the crystalline phase transformation of iPP. It was proved that the β-crystal form of iPP is a thermodynamically metastable structure and will gradually transform to a new kind of α'-crystal form with the rise in crystallization temperature. Because of different structural characteristics, the polymeric nucleating agents exhibit nucleation and crystallization mechanism which differ from the traditional low molecular weight β-nucleating agents of iPP.

1. Introduction

Isotactic polypropylene possesses some features that are unique to semicrystalline polymers. This polymer is of polymorphic composition, having at least four modifications: α, β, γ, and smectic.[1−6] The chain conformation of each modifications is the classical 3_1 helix. The difference in the crystallography is the manner in which the chains are packed in the unit cell. The difference in the crystal forms of iPP has a dramatic impact on the properties of polymer products. Among all the crystal forms of iPP, the β one has many performance characteristics, such as improved elongation at break and impact strength, so in the past few decades much attention has been paid to investigate and elevate the performance of the β-iPP.[7−17]

Since the nucleation of metastable β-crystal form occurs much more rarely in bulk crystallization than that of the predominant α-modification, it can only be obtained through special crystallization procedures, such as in a temperature gradient,[7,8] adding specific nucleating agent,[9−12] or shear-induced crystallization,[13−17] of which the most effective and accessible method to obtain iPP with higher level of β-crystal form is the addition of some β-nucleating agents. However, until now only two classes of compounds have been mainly used as β-nucleating agents: the first class is a minority of aromatic ring compounds, such as γ-quinacridone (Dye Permanent Red E3B), triphenodithiazine, and *N*,*N*-dicyclohexylterephthalamide; the second class includes certain group IIA metal salts or their mixtures with some specific dicarboxylic acids, such as calcium salt of imido acids and compounds of calcium stearate and pimelic acid.[18]

Understanding the nucleation mechanism of β-nucleating agents is a key to improve the properties of iPP, yet only few articles dealt with the nucleation and crystallization mechanism of β-iPP in the past. Lotz and co-workers[10,12,19−21] proposed a "dimensional lattice matching theory" through analyzing the structural relationships between nucleating agents and β-iPP. Their theory can be summarized as the following: a lattice matching between the *c*-axis periodicity of iPP (6.5 Å) and a corresponding distance in the substrate crystal face of nucleating agent is the main reason to induce the β-iPP polymorph. However, the "dimensional lattice matching theory" cannot be applied to all β-nucleating agents, and the nucleation and crystallization mechanism of β-iPP are still not well-understood until now.

Generally speaking, the β-nucleating agents of iPP are crystallizable organic compounds with low molecular weight. Though a higher content β crystal form can be obtained in the blends of iPP with some polymers (such as polyamide-6,[22−25] maleated elastomer,[26−28] ultrahigh-molecular-weight polyethylene,[29,30] etc.) under shear conditions, these polymers are not considered as β-nucleating agents of iPP for they cannot generate β-crystal form during quiescent melt crystallization. Recently, Torre et al.[31] researched the melting behavior of liquid crystalline polymer/iPP blends and found that the liquid crystalline polymer (Vectra A950) can induce both α- and β-nucleation during isothermal crystallization. According to our investigation, some polymers with benzene rings (such as SAN and PS) can also induce the β-iPP polymorph during quiescent isothermal crystallization and improve the impact strength of iPP remarkably. Compared with the traditional β-nucleating agents of iPP, these polymeric nucleating agents boasted some unique structural characteristics and nucleating activity. Their nucleation mechanism cannot be explained by the "dimensional lattice matching theory". Furthermore, as special β-nucleating agents, these polymers have many excellent performances (such as cheapness,

* Corresponding author: Fax +86-10-62770304; e-mail yujian03@mail.tsinghua.edu.cn.

10.1021/ma0623587 CCC: $37.00
Published on Web 05/16/2007

innocuity, easy to process) and exhibit an attractive commercial future. The purpose of this paper is to present some detailed experimental results about the effect of polymeric nucleating agents (represented by SAN and PS) on the crystallization behavior of iPP and to further discuss the nucleation mechanism of β-nucleating agents.

2. Experimental Section

2.1. Materials and Samples Preparation. The matrix polymer used in this work was commercial grade iPP, S1003, with melt flow index of 2.5 g/10 min, $M_w = 2.8 \times 10^5$g/mol, and melting temperature of 165 °C, produced by Yanshan Petroleum and Chemical Corp., China. The polymeric nucleating agent (PS) was obtained from TaiTa Chemical Corp., with melt flow index of 4 g/10 min. Another polymeric nucleating agent (SAN) was obtained from Mitsubishi Plastics, Inc., Japan, with melt flow index of 2.2 g/10 min. The weight percent of acrylonitrile in SAN copolymer is about 23%. Compounding of iPP with PS or SAN was produced using a corotating twin-screw extruder, operating at a melting temperature of 210 °C. The compounds were blended at a screw speed of 25 rpm. PS or SAN proportions in the blends were 0.3, 0.7, 1, 2, 3, 4, and 5 wt %.

The crystallization procedure and thermal history are prime factors in determining the morphological features and physical−mechanical properties of a given polymer. For sample preparation, it is not sufficient to consider only the crystallization condition, but sample size and shape should also be taken into consideration. For example, the actual thermal history of samples with different thickness varied greatly. In this work, to ensure the consistency of thermal histories of different samples, all the samples with different SAN (or PS) content were first sandwiched between two aluminum flakes and melt-pressed to form a film with a thickness of ca. 100 μm. The compression-molded specimens were then melted at 220 °C and kept for 10 min at this temperature to erase any thermal history. At last, they were rapidly cooled to the crystallization temperature (T_c) and kept at this temperature for 2 h to allow crystallization at T_c. The final samples were then rapidly cooled to room temperature for test. In the various isothermal crystallizations, $T_c = 90$, 100, 110, 120, 130, 140, and 150 °C.

2.2. Measurements. WAXD experiments were conducted with a Panalytical (Holland) X' pert Pro MRD diffractometer (Cu Kα, $\lambda = 0.154$ nm, 40 kV, 40 mA, reflection mode). The experiments were performed with a 2θ range of 10°−30°, at a scanning rate of 2°/min, and a scanning step of 0.02°.

The calorimetric measurements were performed with a Mettler DSC 822e differential scanning calorimeter at different scan rates of 10 °C/min in a flowing N_2 atmosphere, and the sample weight was ca. 10 mg. Indium was used as the standard sample.

For optical microscopy observation, a Nikon type 104 optical microscope was used in this study. The optical microscope was equipped with cross-polarizer, with a camera system (Panasonic wv-CP240/G) incorporated, and a programmable heating stage.

The relative amount of different crystal forms present in these samples was measured from the X-ray diffraction profiles. In iPP WAXD profiles, (110) at $2\theta = 14.1°$, (040) at 16.9°, (130) at 18.5° are the principal reflections of the α-crystal form of iPP while (300) at about 15.9° is the principal reflection of the β-crystal form, and they are considered as the characteristic peaks for α-crystals and β-crystals, respectively. The crystallinity and relative content of different crystal forms of iPP can be calculated from the following equations:[9,14,32]

$$K_\beta = \frac{A_{\beta(300)}}{A_{\alpha(110)} + A_{\alpha(040)} + A_{\alpha(130)} + A_{\beta(300)}} \quad (1)$$

$$X_{all} = 1 - \frac{A_{amorphous}}{\sum A_{amorphous} + A_{crystallization}} \quad (2)$$

$$X_\alpha = (1 - K_\beta)X_{all} \quad (3)$$

$$X_\beta = K_\beta X_{all} \quad (4)$$

where K_β expresses the relative amount of the β-crystal form with respect to the α-crystal form; $A_{\beta(300)}$ represents the area of the (300) reflection peak; $A_{\alpha(110)}$, $A_{\alpha(040)}$, and $A_{\alpha(130)}$ represent the areas of the (110), (040), and (130) reflection peaks respectively; and $A_{amorphous}$ is the area of the amorphous peak. In this work, a curve-fitting soft was used to calculate the peak intensities of WAXD profiles. The deconvoluted peaks can be obtained by using the mixed function of Gauss and Lorentz.

3. Results and Discussion

3.1. Effect of the Concentration and Varieties of Polymeric Nucleating Agent. Figure 1 and Figure 2 show that the WAXD profiles of SAN/iPP and PS/iPP blends with different SAN (or PS) content isothermally crystallized at 110 °C under quiescent conditions. To compare the crystalline structures of different samples, the WAXD profiles all plotted at the same intensity scale. It was observed that the WAXD profile of pure iPP show five obvious peaks at 2θ of approximate values 14.2°, 17.0°, 18.7°, 21.3°, and 22.0° respectively, which correspond to the (110), (040), (130), (131), and (111) reflections. These characteristic diffraction angles indicate that only α-monoclinic crystal form exists in the pure iPP sample. However, in the WAXD profiles of SAN/iPP (or PS/iPP) blends with low SAN (or PS) content, there is an obvious peak at about 15.9° which corresponds to the (300) reflection of β-hexagonal crystal form, indicating β-crystal form exists in these samples.

According to eqs 1 and 2, the relative content of β-crystal form (K_β) and the value of the total crystallinity (X_{all}), calculated from the X-ray diffraction profiles as shown in Figures 1 and 2, are reported in Figure 3 as a function of the content of the polymeric nucleating agents. The calculated results show that the X_{all} values of two series of iPP blends both decrease with the increasing SAN or PS percentage. However, the K_β values of two series of iPP blends first increase with the increasing SAN or PS percentage, reaches a maximum value (when SAN or PS percentage is about 2%), and then decreases with a further increase in the SAN (or PS) percentage. The maximum K_β values of SAN/iPP and PS/iPP are 32% and 27%, respectively. The above results indicate that the SAN (or PS) content influences not only the crystallinity but also the crystalline phase of iPP.

Because the thickness of these sample films (ca. 100 μm) almost equals the diameter of spherulite of iPP, the difference between skin and core structure of these sample films can be ignored in this work. At the same time, because the compression-molded specimens were melted at 220 °C and kept for 10 min at this temperature to erase any thermal history before quiescent isothermal crystallization, there is no possibility of flow-induced orientation in the isothermal crystallization. Therefore, the appearance of β-crystal form in SAN/iPP (or PS/iPP) blends with low SAN (or PS) content can be explained by the β-nucleating activity of the two kinds of polymers. To further verify the β-nucleating activity of the two kinds of polymers, in-situ POM measurement was carried out in this work to observe the isothermal crystallization process of the SAN/iPP blend.

α- and β-crystal forms of iPP are easily distinguished under polarized light microscope, in view of their very different optical properties.[3,19,22] It is well-known that β iPP spherulites are highly birefringent as a result of conventional spherulite architecture, with radiating lamellae and tangential orientation of the mo-

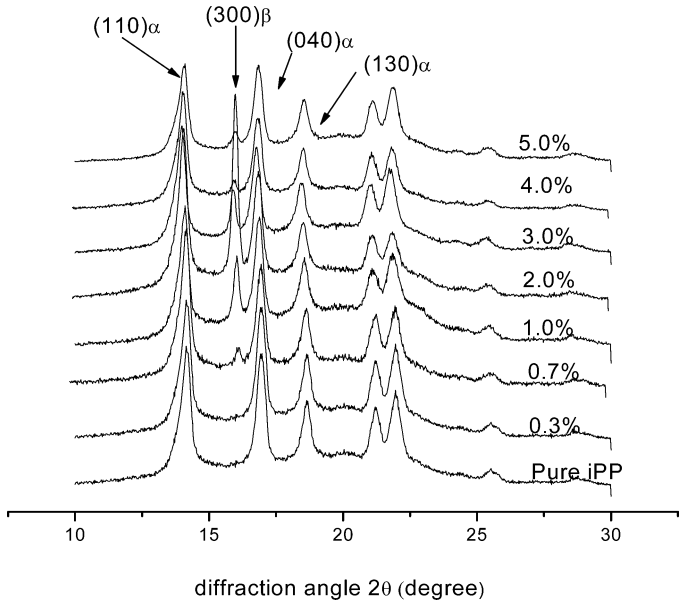

Figure 1. WAXD profiles of SAN/iPP blends with different SAN content isothermally crystallized at 110 °C under quiescent conditions.

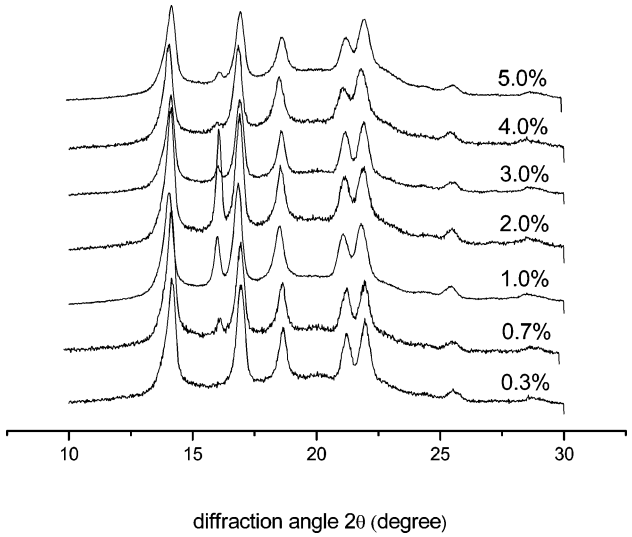

Figure 2. WAXD profiles of PS/iPP blends with different PS content isothermally crystallized at 110 °C under quiescent conditions.

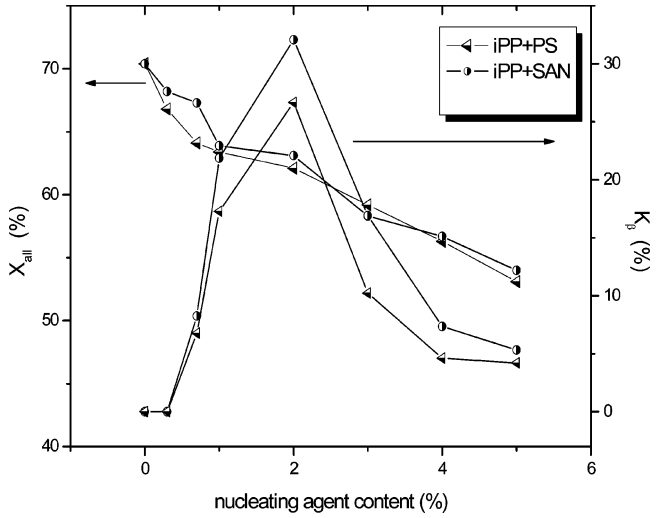

Figure 3. Relative content of β-crystal form (K_β) and the value of crystallinity (X_{all}), evaluated from the X-ray diffraction patterns, in the samples isothermally crystallized from the melt, as a function of the content of the polymeric nucleating agents.

lecular stems in the lamellae. However, α iPP spherulites usually have a much weaker birefringent as a result of a specific mechanism of lamellar branching. Therefore, in the optical micrographs, α-spherulites are darker than β ones.

Figure 4 shows the optical microphotographs of the nucleation and growing process of SAN/iPP blend with 2% SAN during isothermal crystallization at 110 °C. All the optical microphotographs in Figure 4 were taken under cross-polarized light. It can observed that, due to the phase separation between iPP and SAN, SAN assembles to become many microspheres (less than 5 μm) which disperse uniformly in iPP matrix in the early stage of isothermal crystallization. Then with the increasing crystallization time (t_c), some of SAN microspheres begin to induce iPP nucleation (Figure 4a). With further increase in the t_c, both α- and β-crystal form spherulites appear (Figure 4b). The bright spherulite is β-crystal form, and the darker ones are α-crystal forms. In Figure 4c,d, the α- and β-crystal form spherulites gradually grow with the extending t_c until the space was fully occupied.

According to Lotz's investigation,[10] many nucleating agents have dual nucleating activity, and some β-nucleating agents may also induce the α-crystal form during melt crystallization. It is obvious that our investigation proves that SAN and PS are a class of special β-nucleating agent of iPP. They have dual nucleating activity and can induce both α- and β-nucleation in iPP.

In this experiment, DSC, as a basic scientific approach, was also adopted to investigate the special nucleating ability of polymeric nucleating agents. However, in most experimental conditions, compared with the result of WAXD, the signals of β-crystallization peaks in DSC curves are not as significant as it is in WAXD, and some crystalline peaks in DSC curves overlap with each other. Consequently, the calculated results of DSC were not used to investigate the crystalline behavior of polymeric nucleating agents/iPP blends, and the results of DSC are not included in this paper.

Generally speaking, increasing the concentration of the nucleating agents helps to increase the proportion of β-crystal form. However, the results of Figure 3 indicate that the K_β values of two series of iPP blends do not increase linearly with the increasing SAN (or PS) percentage, but reach a maximum value

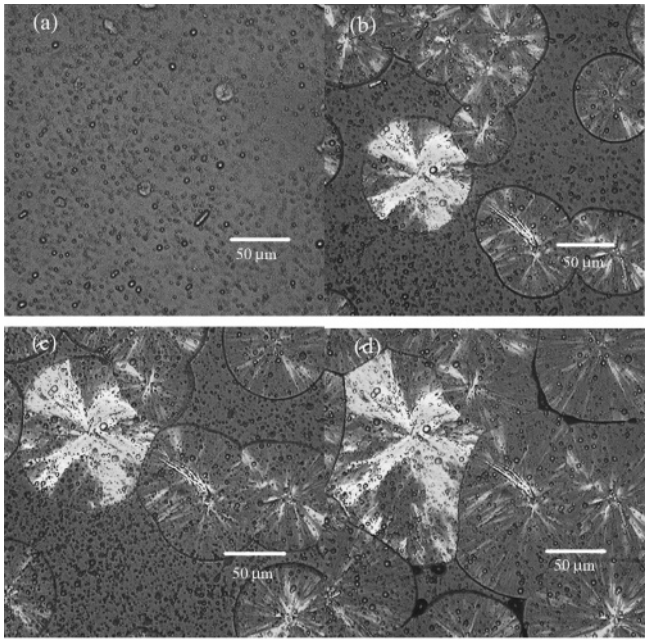

Figure 4. In-situ optical micrographs of the nucleation and growth process of SAN/iPP blend with 2% SAN during isothermal crystallization at 110 °C.

when SAN or PS percentage is about 2%. It can be explained by the changes of dispersibility of polymeric nucleating agents in iPP matrix. The dispersibility of polymeric nucleating agents heavily depends on the concentration of nucleating agents and the mixing method. Under the same conditions, increasing the concentration of the nucleating agents will increase the particle sizes of polymeric nucleating agents and weaken their dispersibility in iPP matrix. At the same time, weakening dispersibility will lower the nucleating efficiency of the polymeric nucleating agents. Consequently, the proportion of β-crystal form does not increase linearly with the increasing SAN (or PS) percentage because of the conflicting relationship between the concentration and the dispersibility.

Figure 5 shows the optical microphotographs of SAN/iPP blends crystallized isothermally at 110 °C. From Figure 5a−c, SAN proportions in the blends were 0.3%, 2%, and 5%, respectively. All the optical microphotographs in Figure 5 were taken by POM without cross-polarized light, and the SAN microspheres in iPP can be observed clearly. It is apparent that, in Figure 5a, only a few SAN microspheres (less than 3 μm) can be observed. As a result, there are not enough nucleating agents to induce the β-iPP polymorph, and thus the α-crystal form is predominantly obtained. When SAN proportion in the blend reaches 2% (Figure 5b), the SAN micospheres disperse uniformly in the iPP matrix, and the size of SAN micospheres does not change significantly, indicating that the dispersibility of SAN does not weaken with the increasing SAN percentage. As a result, the proportion of β-crystal form increases when SAN percentage increasing from 0.3% to 2%. In Figure 5c, when SAN proportion in the blend reaches 5%, the size of the SAN micospheres (ca. 10−30 μm) increases greatly, indicating that the dispersibility of SAN weakens with the increasing SAN percentage. It results in a loss of nucleating efficiency of SAN and the decreasing of the proportion of β-crystal form.

Another interesting phenomenon is that, under the same crystallization condition, SAN is more effective than PS on inducing β-crystal form in iPP. This can be explained by the structural difference of these two kinds of polymers. Some special functional groups (such as nitrile) in SAN may help to

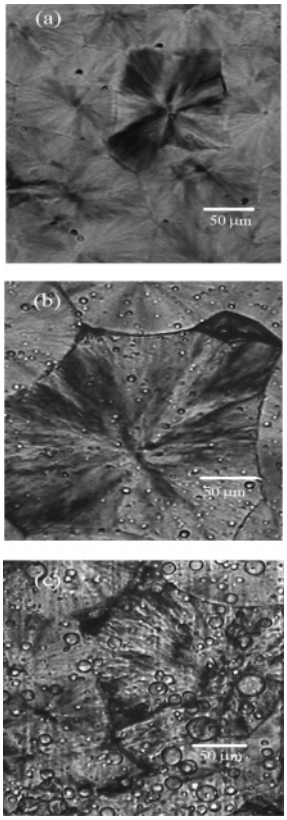

Figure 5. Polarized light microphotographs after isothermal crystallization at 110 °C of the (a) iPP/SAN (99.7:0.3), (b) iPP/SAN (98:2), and (c) iPP/SAN (95:5).

enhance the β-nucleating activity of iPP. All the above analysis and discussion clearly indicate that SAN (or PS) used in this work both have a prominent β-nucleating effect on iPP, and the proportion of β-crystal form is greatly influenced by the concentration and molecular structures of these two kinds of polymers.

Furthermore, in our experiments, through comparing the mechanical ability data (including stretching, bending, impacting strength) of pure iPP and SAN/iPP injection-molding samples, we found that the impact strength of SAN/iPP is obviously improved compared to that of pure iPP. When SAN percentage is about 2%, the maximum impact strength value of SAN/iPP can be enhanced by almost 60%. At the same time, according to the results of WAXD measurement, we found that SAN has significant β-nucleating ability and the β-form content in SAN/iPP is higher than that of pure iPP. These results indicated that SAN help to enhance the β-form content of iPP and improve the mechanical properties of iPP samples.

3.2. Effect of the Crystallization Temperature (T_c). Different thermal histories have great influence on the β-nucleating ability of the polymeric nucleating agents, which in turn will influence the phase structure of iPP samples. On the basis of the above research results, we adopt SAN/iPP and PS/iPP blends with 2% SAN (or PS) percentage to investigate the influence of crystallization temperature on the final condensed structure of iPP.

The WAXD profiles of SAN/iPP and PS/iPP blends with 2% SAN (or PS) isothermally crystallized from melt at different temperatures are shown in Figure 6 and Figure 7, respectively. The crystallization time of these samples is 2 h. The K_β values, calculated from the X-ray diffraction profiles in Figures 6 and 7, is reported in Figure 8 as a function of the crystallization temperature. It was observed that the β-crystal form only can

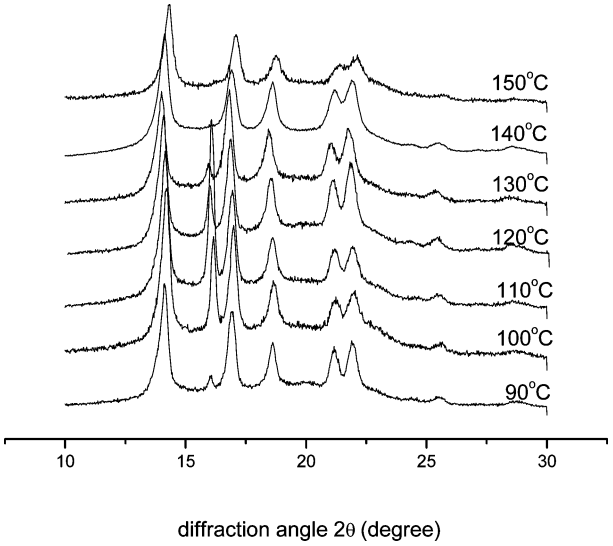

Figure 6. WAXD profiles of SAN/iPP blends with 2% SAN isothermally crystallized at the indicated crystalline temperatures.

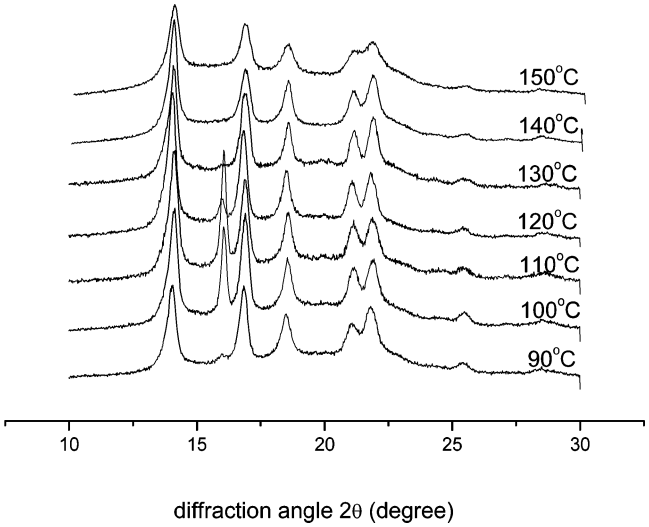

Figure 7. WAXD profiles of PS/iPP blends with 2% PS isothermally crystallized at the indicated crystalline temperatures.

be obtained in a certain temperature range (from 90 to 130 °C). The K_β values increases with the rise in crystallization temperature, reaches a maximum when T_c is about 110 °C, and then decreases with a further rise in T_c. At the same crystallization temperature, SAN is more effective than PS on inducing β-crystal form in iPP. The changing pattern of K_β value in Figure 8 is similar to that of Figure 3.

On the basis of such complex polymorphic behavior of SAN/iPP and PS/iPP blends, the reason for the presence of the maxima in the curves of the content of β crystal form as a function of the crystallization temperature may be explained as the result of two competing kinetic and thermodynamic effects. Lotz et al.[10,33−35] have proved that the growth rate of β phase is considerably faster than that of the α-phase in the conventional crystallization temperature range of iPP (i.e., between 100 and 140 °C). Therefore, for the present samples of iPP, blending with an appreciable amount of SAN (or PS), the formation of the β crystal form is thermodynamically favored in the temperature range from 100 to 140 °C. Consequently, with the increasing crystallization temperature the amount of β-crystal form increases, but at higher crystallization temperatures the crystallization of metastable β-crystal form is too slow because of its lower melting temperature, and the more stable α-form

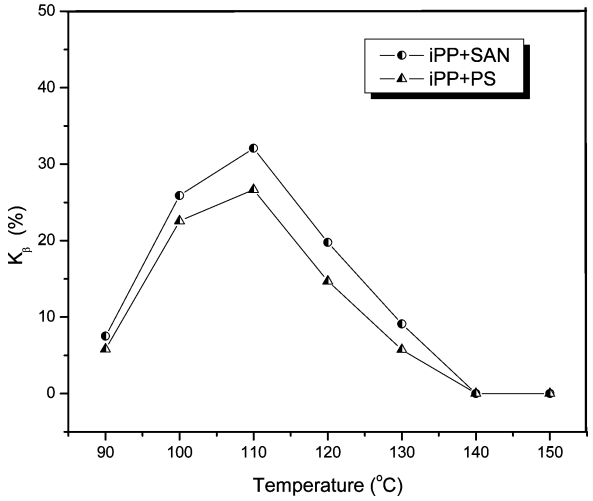

Figure 8. Relative content of β-form crystal (K_β), evaluated from the X-ray diffraction patterns, in the samples isothermally crystallized from the melt, as a function of the crystallization temperature.

becomes again kinetically favored, so that the amount of β-crystal form decreases.

The results of the above analysis indicate that the samples of SAN/iPP and PS/iPP blends crystallize from the melt in mixtures of crystals of α- and β-forms. Different crystalline temperature will influence the final condensed structure of iPP.

3.3. Transformation between Different Crystalline Phases. As mentioned above, the polymeric nucleating agents (SAN or PS), dispersing within iPP matrix, may act as β-nucleating agents and induce the β-iPP polymorph. The β-crystal form of iPP is a metastable phase, and it will transform to the stable α-phase under special conditions. Since the first report on the phase transformation in β-iPP by Padden and Keith,[6] the structural changes involved in the transformation have been widely studied, and a number of mechanisms on $\beta-\alpha$ transformation have been established.[19,36−38] However, these phenomena are still under debate. To better understand the polymorphism of the polymeric nucleating agent/iPP blends, the phase transformation between different crystal forms was also investigated by variable temperature WAXD and POM experiments in this work.

The WAXD profiles of a sample of iPP with 2% SAN were recorded at different melting temperatures after quiescent melt crystallization at 110 °C for 2 h, which are shown in Figure 9. The melting temperatures were selected according to the positions of melting peaks in the DSC scans of SAN/iPP blends. It was observed that the variation of the intensities of different crystalline peaks is distinct with the increasing temperature. According to the eqs 1−4, the total crystallinity of iPP (X_{all}) and the crystallinity of different crystal forms (X_α and X_β) can be calculated (Figure 10). It can be seen that the values of X_{all} and X_β both decrease with the rise in the melting temperature, while X_α first increases with the rise in the melting temperature, reaching a maximum amount at 147 °C, and then decreases with a further rise in the melting temperature. The results indicate that the phase transformation between β and α form takes place in the process of heating.

Figure 11 shows the variation of the X_α value of SAN/iPP blend with 2% SAN content, calculated from the WAXD profiles of Figure 8, as a function of the melting temperature and the DSC heating thermogram of the SAN/iPP blend. The DSC thermogram clearly show multiple endothermic peaks which can be assigned to the melting of the different crystal forms of iPP[39] or recrystallization and reorganization of the

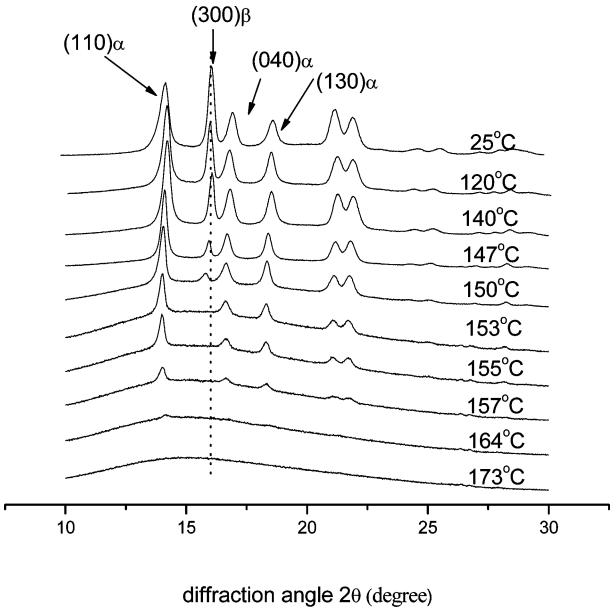

Figure 9. Variable temperature WAXD profiles of SAN/iPP blend with 2% SAN after quiescent melt crystallization at 110 °C for 2 h.

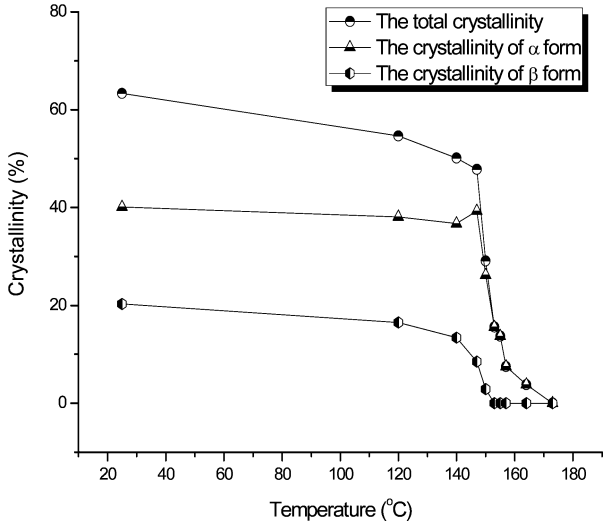

Figure 10. Variation of crystallinity of different crystal forms with increasing temperature. The data were obtained from WAXD measurements.

imperfect crystal forms during heating.[40] The two melting peaks (at 150 and 164 °C) in Figure 11 correspond to the β-form and α-form, respectively. The endothermic peak (155 °C) is caused by the melting of less stable α′-crystal forms that had formed during the initial stages of the heating process via $\beta-\alpha$ recrystallization within the β-phase. Comparing the variation of the X_α obtained from the variable temperature WAXD data with the DSC heating thermogram of the SAN/iPP blend, it can be observed that X_α reaches a maximum value when β-melting peak begins to disappear. It means the phase transformation takes place at the melting temperature of β-crystal form. The newly formed α′-crystal form is less stable crystal form and will melt at lower melting temperature. This phenomenon also can be proved by variable temperature POM measurement.

The morphology of the SAN/iPP blend developed in the process of heating was analyzed by polarized optical microscopy. Figure 12 shows the variable temperature polarized light micrographs of the SAN/iPP blend after quiescent melt crystallization at 120 °C for 2 h. It is evident that both α- and β-crystal

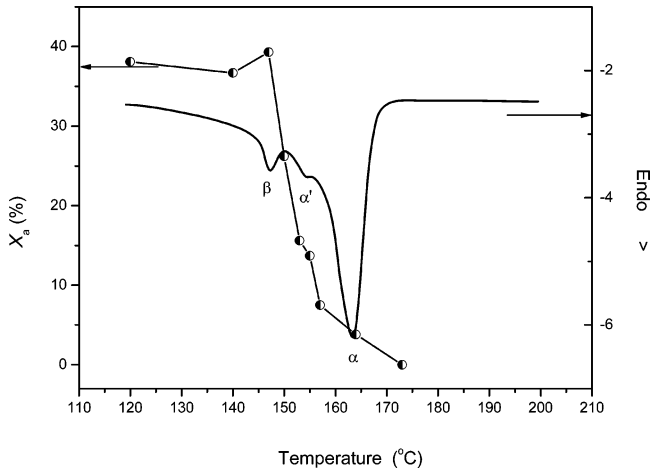

Figure 11. Variation of the X_α value of SAN/iPP blend with 2% SAN, calculated from the WAXD profiles of Figure 8, as a function of the melting temperature. Comparing with the DSC heating thermogram of SAN/iPP blend with 2% SAN.

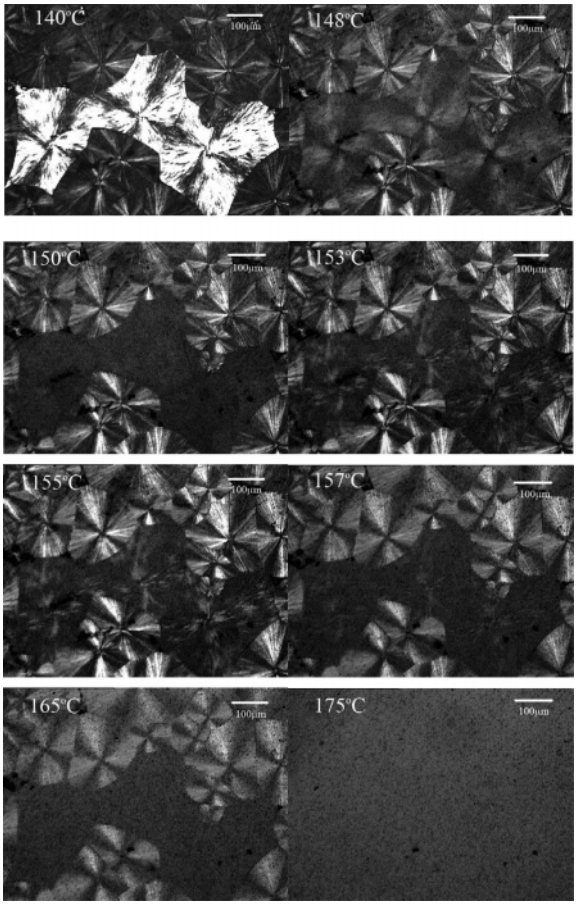

Figure 12. Variable temperature polarized light microphotographs of SAN/iPP blend after quiescent melt crystallization at 120 °C for 2 h.

form spherulites may be observed in the SAN/iPP blend. The β-crystal form spherulites melt gradually with the increasing temperature and then disappear completely at 150 °C. Nevertheless, a new crystalline phase comes into being within the β-phase with a further rise in the melting temperature (153 °C). The newly formed crystalline phase is positive spherulites with lower melting temperature. It begins to melt at 155 °C and disappears completely at 165 °C. Combined the results of DSC, the newly formed crystalline phase within the β-phase can be defined as a less stable α′-crystal form. The phase transformation between α- and β-phases is a melting and recrystallization process.

It is known that both α- and β-phases of iPP are based on the same 3-fold helical conformation of the molecular chains. As a result, growing transitions between the two crystal forms are structurally feasible. Increasing the melting temperature induces the rearrangement of 3_1 helical chains of iPP and consequently causes the gradual transformation from β to α crystal form. Compared with isothermal crystallization process, the time of melting and recrystallization of β crystal form on heating process is too short for the helical chains of iPP to adjust them to a stable state. As a result, the newly formed crystalline phase (α′) is less stable than the α-crystal form.

3.4. Structural Requirement for the Polymeric Nucleating Agent. Analysis of the structural relationships between the polymeric nucleating agents and β-crystal form helps establish, at least in their broad outlines, the structural requirements these nucleating agent must meet. Different from the α-crystal form, the β-crystal form has a highly unusual crystal structure, with a trigonal unit cell in which three isochiral helices adopt a frustrated packing.[41] It does not comply with the rules of classical crystallography which postulate structural equivalency. Indeed, the helices of β-crystal form have different azimuthal orientations since the corner chains are rotated by ∼180° (or, in view of the 3-fold symmetry of the helices, by ∼60°) relative to the middle chains. Different nucleating agents can induce these helical chains organizing into several different spatial arrangements and giving rise to distinct polymorphs.

According to our investigation, the polymers with β-nucleating activity all have benzene rings in their molecular structure (such as PS or SAN). The benzene rings of the polymeric nucleating agents may act as a growth surface of crystal and induce the helix chains of iPP epitaxial crystallize on it. SAN is more effective than PS on inducing higher level of β-crystal form in iPP under the same crystallization condition, indicating that some polar functional groups (such as nitrile) may enhance the β-nucleating activity of iPP.

It should be pointed out that both SAN and PS, different from traditional β-nucleating agents of iPP, show unique structural characteristics (both chain structure and condensed state structure). First, they are both macromolecules with special functional groups. Second, they are amorphous polymers and cannot form special crystalline structure to match the β-iPP chain axis repeat distance. Therefore, the nucleation mechanism of the polymeric nucleating agents cannot be explained by the "dimensional lattice matching theory".

4. Conclusion

In the current study, the influences of SAN and PS on the crystallization behavior of iPP have been investigated. A different polymorphic behavior has been observed between the polymeric nucleating agents/iPP blends and pure iPP under the same thermal treatment. Whereas pure iPP crystallized in the α-modification, the crystallization of the polymeric nucleating agents/iPP blends with a low SAN (or PS) content were characterized by the appearance of both α- and β-crystal forms. It is apparent that both SAN and PS used in this work have a prominent β-nucleating effect on iPP. They are a class of special β-nucleating agents of iPP. They have dual nucleating activity and can induce both α- and β-nucleation in iPP simultaneously.

The nucleating activity of SAN and PS showed significant dependence on concentration, molecular structures, and crystallization temperature. The proportion of β-crystal form in those two series of iPP blends increase with the increasing SAN (or PS) content, reaches a maximum value, and then decreases with a further increase in the (SAN or PS) content. The significant reduction of the β-crystal form could be explained by the changes of dispersibility of polymeric nucleating agents in iPP matrix. SAN is more effective than PS on inducing higher level of β-crystal form in iPP under the same crystallization condition. This can be explained by the structural difference of two kinds of polymers. Polar functional groups (such as nitrile) in SAN may help to enhance the β-nucleating activity of iPP.

Different thermal histories also have great influence on the β-nucleating ability of SAN and PS. The β-crystal form can only be obtained in a certain temperature range (from 90 to 130 °C). The β-form content increases with the rise in crystallization temperature, reaches a maximum for T_c at 110 °C, and then decreases with a further rise in T_c. The presence of the maxima in the curves of the content of β-form as a function of the crystallization temperature may be explained as the result of two competing kinetic and thermodynamic effects.

With obvious evidence of variable temperature WAXD and POM experiments, it was proved that the β → α phase transformation takes place with the rise in melting temperature. The phase transformation between β- and α-crystal form is a melting and recrystallization process. The newly formed crystalline phase is a less stable α′-crystal form and is produced during the initial stages of the heating process via melt and recrystallization within the β-phase.

Different from traditional β-nucleating agents of iPP, these polymeric nucleating agents present unique structural characteristics and nucleating activity. They are amorphous polymers, and their nucleation mechanism is different from that of the traditional nucleating agents.

Acknowledgment. The authors are grateful to Prof. D. J. Wang for insightful discussions and interpretations of the results. The experimental assistance by Prof. R. Yang and Prof. J. Xu is greatly appreciated. The financial support from Postdoctor Science Foundation of China (Grant No. 023101067) is also greatly acknowledged.

References and Notes

(1) Morrow, D. R.; Newman, B. A. *J. Appl. Phys.* **1968**, *39*, 4944.
(2) Turner-Jones, A.; Cobbold, A. J. *J. Polym. Sci.* **1968**, *B6*, 539.
(3) Bruckner, S.; Meille, S. V. *Nature (London)* **1989**, *340*, 455.
(4) Meille, S. V.; Bruckner, S.; Porzio, W. *Macromolecules* **1990**, *23*, 4114.
(5) Lotz, B.; Graff, S.; Straupe, C.; Wittmann, J. C. *Polymer* **1991**, *32*, 2902.
(6) Padden, F. J.; Keith, H. D. *J. Appl. Phys.* **1959**, *30*, 1479.
(7) Fujiwara, Y. *Colloid Polym. Sci.* **1975**, *253*, 273.
(8) Lovinger, A. J.; Chua, J. O.; Gryte, C. C. *J. Polym. Sci., Polym. Phys. Ed.* **1977**, *15*, 641.
(9) Huo, H.; Jiang, S. C.; An, L. J.; Feng, J. C. *Macromolecules* **2004**, *37*, 2478.
(10) Stocker, W.; Schumacher, M.; Graff, S.; Thierry, A.; Wittmann, J. C.; Lotz, B. *Macromolecules* **1998**, *31*, 807.
(11) Vaga, J. *J. Therm. Anal.* **1989**, *35*, 1891.
(12) Mathieu, C.; Thierry, A.; Wittmann, J. C.; Lotz, B. *J. Polym. Sci., Part B: Polym. Phys.* **2002**, *40*, 2504.
(13) Somani, R. H.; Hsiao, B. S.; Nogales, A.; Srinivas, S.; Tsou, A. H.; Scics, I.; Balta-Calleja, F. J.; Ezquerra, T. A. *Macromolecules* **2000**, *33*, 9385.
(14) Somani, R. H.; Hsiao, B. S.; Nogales, A.; Fruitwala, H.; Srinivas, S.; Tsou, A. H. *Macromolecules* **2001**, *34*, 5902.
(15) Jay, F.; Haudin, J. M.; Monasse, B. *J. Mater. Sci.* **1999**, *34*, 2089.
(16) Tribout, C.; Monasse, B.; Haudin, J. M. *Colloid Polym. Sci.* **1996**, *274*, 197.
(17) Varga, J. *Angew. Makromol. Chem.* **1983**, *112*, 191.
(18) Chen, H. B.; Karger-Kocsis, J.; Wu, J. S.; Varga, J. *Polymer* **2002**, *43*, 6505.
(19) Lotz, B. *Polymer* **1998**, *39*, 4561.
(20) Wittmann, J. C.; Lotz, B. *Prog. Polym. Sci.* **1990**, *15*, 909.
(21) Mathieu, C.; Thierry, A.; Wittmann, J. C.; Lotz, B. *Polymer* **2000**, *41*, 7241.

(22) Boucher, E.; Folkers, J. P.; Creton, C.; Hervet, H.; Leger, L. *Macromolecules* **1997**, *30*, 2102.
(23) Garbarczyk, J.; Paukszta, D.; Borysiak, S. *J. Macromol. Sci., Part B: Phys.* **2002**, *41*, 1267.
(24) Liu, X.; Wu, Q. J.; Burglund, L. A.; Fan, J. Q.; Qi, Z. N. *Polymer* **2001**, *42*, 8235.
(25) Feng, M.; Gong, F. L.; Zhao, C. G.; Chen, G. G.; Zhang, S. M.; Yang, M. S.; Han, C. C. *J. Polym. Sci., Part B: Polym. Phys.* **2004**, *42*, 3428.
(26) Di, Y. W.; Iannace, S.; Nicolais, L. *J. Appl. Polym. Sci.* **2002**, *86*, 3430.
(27) Varga, J. *Thermal Anal.* **1989**, *35*, 1891.
(28) Varga, J.; Garzo, G. *Angew. Makromol. Chem.* **1990**, *180*, 15.
(29) Wang, K. J.; Zhou, C. X. *Polym. Eng. Sci.* **2001**, *41*, 2249.
(30) Varga, J.; Schulek, T. F.; Mudra, I. *Macromol. Symp.* **1994**, *78*, 229.
(31) Torre, J.; Cortazar, M.; Gomez, M.; Ellis, G.; Marco, C. *J. Polym. Sci., Part B: Polym. Phys.* **2004**, *42*, 1949.
(32) Turner-Jones, A.; Aizlewood, J. M.; Beckett, D. R. *Makromol. Chem.* **1964**, *75*, 134.
(33) Lotz, B.; Fillon, A.; Thierry, A.; Wittmann, J. C. *Polym. Bull. (Berlin)* **1991**, *25*, 101.
(34) Norton, D. R.; Keller, A. *Polymer* **1985**, *26*, 704.
(35) Varga, J. In *Poly(propylene*): *Structure, Blends and Composites*; Karger-Kocsis, J., Ed.; Chapman & Hall: London, 1995; Vol. 1, Chapter 3, pp 56−115.
(36) Varga, J.; Toth, F. *Makromol. Chem., Macromol. Symp.* **1986**, *5*, 213.
(37) Meille, S. V.; Ferro, D. R.; Bruckner, S.; Lovinger, A. J.; Padden, F. J., Jr. *Macromolecules* **1994**, *27*, 2615.
(38) Dorset, D. L.; McCourt, M. P.; Kopp, S.; Schumacher, M.; Okihara, T.; Lotz, B. *Polymer* **1998**, *39*, 6331.
(39) Marco, C.; Gomez, M. A.; Ellis, G.; Arribas, J. M. *J. Appl. Polym. Sci.* **2002**, *86*, 531.
(40) Yadav, Y. S.; Jain, D. C. *Polymer* **1986**, *27*, 721.
(41) Lotz, B.; Wittmann, J. C.; Lovinger, A. *Polymer* **1996**, *37*, 4979.

MA0623587